SSJR-Net: Semi-Supervised Few-Shot Radar Jamming Recognition Network

Zhenyu Luo, Yunhe Cao, *Member, IEEE,* Tat-Soon Yeo, *Life Fellow, IEEE,* Yulin Zhang, Meiguo Gao

***Abstract*—Deep learning-based radar jamming recognition focuses on identifying the jamming types by using the convolutional neural network (CNN). Though achieving superior performance in recent years, existing deep learning-based few-shot methods are still unable to break through the barrier of needing at least 5% labeled data for supervised learning, and fail to utilize the large amounts of unlabeled data. Considering the difficulty and formidable cost of acquiring labeled data and the ease of acquiring large amounts of unlabeled data in real scenarios, it is meaningful to explore a semi-supervised jamming recognition method by utilizing fewer labeled data and extensive unlabeled data. To this end, a few-shot semi-supervised radar jamming recognition network via a self-training framework is proposed in a challenging setting (1% labeled data, 5 labeled data for each jamming class). To effectively mine the recognition-related knowledge from the labeled data, a mutual learning strategy is first proposed by constraining the consistency between the predictions on original jamming data and their augmented data. With the trained mutual learning strategy, the pseudo-labels of unlabeled data can be obtained by taking the unlabeled jamming data as input. Then, to select more reliable pseudo-labeled data, a pseudo-labeled samples selection mechanism is proposed by introducing confidence scores to filter the high-quality pseudo labels. With the two above mentioned components, our framework is able to effectively exploit information contained in both labeled and unlabeled data through self-training in a semi-supervised manner. Extensive experiments on dataset with a mixture of simulated and measured data demonstrate that the proposed semi-supervised jamming recognition method (SSJR-Net) outperforms the state-of-the-art techniques in few-shot jamming recognition and semi-supervised recognition.**

***Index Terms*—Few-shot radar jamming recognition, mutual learning strategy, pseudo-labeled samples selection mechanism, semi-supervised learning**

I. Introduction

WITH the rapid advancement of electronic warfare technology, the electromagnetic environment for radars is becoming increasingly complex and challenging, and jamming has become a big threat to radar target detection, tracking and weapon system guidance [1–3]. Therefore, improving the anti-jamming capability of radar in complex environments is now a hot research topic [4, 5]. Jamming recognition, as the first and critical step in anti-jamming technology, has drawn significant attention in recent years [6, 7].

Jamming recognition research can be classified into methods based on manual feature extraction [8–16] and deep learning (DL) [17–23]. For example, Su et al. [15] extracted both time and frequency domain characteristics of the jamming signal and classified them with the pre-designed classifier. In [16], the type of jamming signal was recognized by extracting the characteristic parameters in the fractional domain of the jamming. He et al. [4] designed a variable polarization anti-jamming method based on the polarization invariant. However, these methods based on manual feature extraction are usually laborious and time-consuming.

Motivated by the significant feature extraction advantages of deep learning, particularly the convolutional neural network (CNN), an increasing number of DL-based methods are proposed to address the limitations of traditional jamming recognition methods [20]. For example, Yu et al. [21] introduced a DL-based method for the detection and classification of barrage jamming in synthetic aperture radar systems. In [22], a robust power-spectrum feature-based jamming recognition network was proposed for the recognition of ten suppressive jamming signals. Yang et al. [23] proposed a fuzzy jamming signal detector combines time-frequency analysis with network model. Even though these DL-based jamming recognition methods eliminate the demand for expert-driven feature extraction in traditional methods, they still require substantial labeled data for training. While in practical scenarios, obtaining a large quantity of accurately labeled samples is expensive in terms of both time and manpower.

In recent years, few-shot recognition methods have been developed to alleviate the above problems [24–33]. Lin et al. [24] introduced a novel architecture aimed at mitigating overfitting in cases of limited data. Zhang et al. [25] providing a new solution to fine-grained signal modulation recognition. Wu et al. [26] proposed a label-guided denoising diffusion probabilistic model and achieved accurate few-shot jamming recognition based on data augmentation. In [29], a few-shot recognition method based on time-frequency self-attention and global knowledge distillation (JR-TFSAD) is designed. Although these methods alleviate the requirement for extensive high-quality labeled samples in jamming recognition, they often still need to annotate at least 5% of jamming samples and ignore the recognition-related knowledge from unlabeled data, thus hindering recognition performance. In this paper, we focus on developing a semi-supervised method in a more challenging setting (*i.e.*, 1% labeled data), which aims to eliminate the reliance on extensive labeled data while jointly utilizing the unlabeled data to further enhance the recognition performance. The key insight behind this work is to design a method to dig and exploit the recognition-related knowledge from the labeled data, while further extending the knowledge to the learning of unlabeled data to improve the recognition

Corresponding author: Yunhe Cao: caoyunhe@mail.xidian.edu.cn; Meiguo Gao: meiguo_g@bit.edu.cn

Zhenyu Luo, Meiguo Gao are with the School of Information and Electronics, Beijing Institute of Technology, Beijing 100081, China.

Yunhe Cao, Yulin Zhang are with the National Key Laboratory of Radar Signal Processing, Xidian University, Xi'an 710071, China.

Tat-Soon Yeo is with the Department of Electrical and Computer Engineering, National University of Singapore, 119077, Singapore.

performance for radar active jamming. On the one hand, there is an urgent need to investigate a method that is capable of mining discriminative and robust features in the face of extremely scarce labeled data. On the other hand, considering that the unlabeled data may still contain useful recognition-related knowledge while lacking the corresponding labels for training the network, the most important step is to obtain reliable labels for the unlabeled data to further assist in the network training. Theoretically, if there is a jamming recognition network trained by existing labeled jamming signals, then pseudo-labels can be generated by taking the unlabeled data as input. Subsequently, the pseudo-labels are capable of further improving the performance of the recognition network with the support of the labeled data.

The main contributions behind this work are summarized as follows.

1) By considering the complexity and diversity of radar active jamming as well as the scarcity of labeled jamming samples, a novel semi-supervised radar jamming recognition network is proposed to recognize jamming signal under a more challenging few-shot setting (5 labeled samples for each class).

2) To effectively mine the recognition-related knowledge behind small amount of labeled jamming samples, a mutual learning strategy (MLS) is designed by explicitly constraining the consistency of predictions. Thanks to MLS, the model is capable of obtaining more stable predictions, thus generating the corresponding pseudo-labels for unlabeled samples.

3) To further obtain reliable and accurate pseudo-labeled jamming samples for explore the recognition-related knowledge from unlabeled jamming data, the pseudo-label selection mechanism (PLSM) is designed by selecting high-confidence pseudo-labeled samples assisting in training, thus further boosting the recognition performance.

4) Extensive experiments on both simulated and measured mixed dataset demonstrate the superior performance of the proposed method over existing few-shot supervised learning and semi-supervised recognition methods.

The organization of the paper is as follows. Section II discusses the related literature. Section III presents the preparation of the dataset required for the experiments. The proposed SSJR-Net is detailed in Section IV. In Section V, we focus on the experimental details and results, along with a comprehensive analysis of the results. Finally, Section VI concludes the paper and provides a summary of the whole work.

II. Related Work

A. Few-shot Learning

Few-shot learning proposes a promising solution to overcome the data scarcity issue in jamming recognition. Wang and Zhai [33] proposed prototypical siamese networks for few-shot learning. Shao et al. [27] developed a deep siamese network to alleviate the poor jamming recognition in few-shot conditions. Lv et al. [28] proposed a weighted ensemble CNN incorporating transfer learning to recognize radar deception jamming. Wu et al. [26] developed a label-guided denoising diffusion probabilistic model incorporating data augmentation, achieving accurate jamming recognition, particularly for compound jamming recognition with limited data. Luo et al. [29] achieved accurate few-shot jamming recognition through the time-frequency self-attention and global knowledge distillation model. Liu et al. [30] designed a distributed architecture to achieve few-shot communication jamming recognition based on foreground segmentation. Besides, Zhang et al. [25] tackled the problem of working mode recognition of multifunction radar throuth a few-shot learning method based on compound alignments. However, the previous few-shot recognition methods still rely on several labeled samples while ignoring the beneficial information of the extensive easily available unlabeled samples.

B. Semi-supervised Learning

Recently, to ease the cost paid by the numerous labeled data, semi-supervised learning methods have been proposed to address problems in natural image processing [34–41]. By introducing Kullback-Leibler (KL) divergence loss and sparsity-promoting cross-entropy loss, the method in [37] achieves a promising performance in semi-supervised signal recognition tasks. In [39], a semi-supervised recognition method incorporating bias-variance decomposition and attention mechanism is presented. Additionally, generative adversarial networks (GANs) are widely used to solve semi-supervised problems due to their data generation and feature representation abilities. To explore the useful information of the unlabeled data, a simple solution is to directly transfer those methods to jamming recognition. However, this solution mainly faces some challenges. First, the type of the data is different between the natural image processing and jamming recognition. When the labeled sample size decreases and the complexity of the jamming environment increases, the recognition accuracy of the aforementioned methods decreases significantly. Second, the limitations of these semi-supervised learning-based methods include incomplete mining of useful information in labeled samples or poor reliability of the generated pseudo-labels, thus limiting the performance of the jamming recognition. To this end, it is important to develop a semi-supervised method for few-shot radar active jamming recognition.

III. Signal Model and Dataset Preparation

A. Signal model

The received signal $S_r(t)$ includes the target echo $S(t)$, the jamming signal $J(t)$ and the internal noise $n(t)$, which can be expressed as

$$S_r(t) = S(t) + J(t) + n(t) \tag{1}$$

where $0 \le t \le T$, T represents a pulse repetition period. And it is usually assumed that $n(t)$ is a white noise signal obeying Gaussian distribution [42].

Radar active jamming generally be categorized into suppressive jamming [43] and deceptive jamming [44] based on their respective effects. Suppressive jamming uses noise as the source of jamming, and the jammer modulates the high-energy noise to drown out the target echo and affect the normal operation of the radar. Deceptive jamming relies on

This article has been accepted for publication in IEEE Transactions on Aerospace and Electronic Systems. This is the author's version which has not been fully edited and content may change prior to final publication. Citation information: DOI 10.1109/TAES.2025.3578404

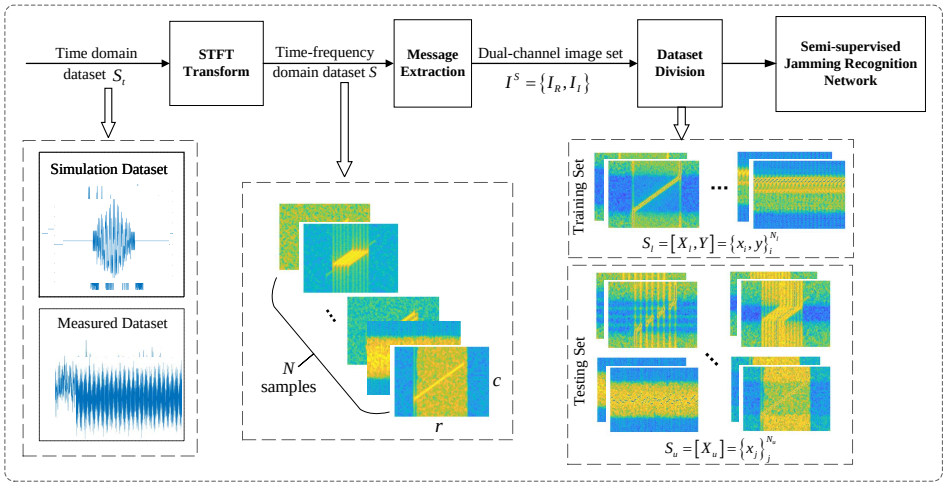

Fig. 1. The process for dataset construction and allocation.

digital radio frequency memory (DRFM), which generates false targets to disrupt the radar's line of sight and disrupt the its normal working state. Moreover, some forms of noise-modulated deceptive jamming can mimic the effects of suppression jamming. Recently, new types of active jamming have emerged. Some typical jamming signals are described below.

a) Blocking Jamming (BJ): Blocking jamming [43] is the most basic form of suppressive jamming, which can be applied in the case of unknown target radar parameters, so it requires less accuracy in frequency guidance equipment. In addition, blocking jamming has a wide enough bandwidth to cover multiple frequency bands at the same time, so it can interfere with radars of most regimes. BJ is usually generated by a noise amplitude-modulated signal, which has the following time-domain expression

$$J_{BJ}(t) = [u_0 + n(t)] \cdot \cos(2\pi f_0 t + \varphi) \tag{2}$$

where $n(t)$ represents a Gaussian white noise with mean 0 and variance σ^2 , u_0 and center frequency f_0 are constant, phase φ uniformly distributed in $[0, 2\pi]$.

b) Distance Deception Jamming (DDJ) : The jammer outputs deceptive targets of varying ranges by controlling the delay time of the DRFM forwarding radar transmit signals. For a realistic deception jamming effect, DDJ [44] is typically modulated only in amplitude with time domain form as

$$J_{DDJ}(t) = A_J \cdot S(t - t_0 - \tau_0) \tag{3}$$

where A_J denotes jamming amplitude, t_0 and τ_0 indicate the delays in the true target echo and the jammer's signal forwarding, respectively.

c) Dense False Target Jamming (DFTJ): DFTJ [45] an extension of DDJ, where the jammer forwards multiple copies of the signal stored in the DRFM in a single pulse repetition cycle, thus forming a dense cluster of multiple false targets, which will consume radar resources and have a certain suppression effect. It has the following time-domain expression

$$J_{DFTJ}(t) = \sum_{m=1}^{M} A_m \cdot S(t - t_0 - \tau_m) \tag{4}$$

where M is the forwarding times of the jammer, A_m is the modulation amplitude of the *mth* false target, t_0 and τ_m represent the delay of the real target echo and the *mth* false target, respectively. DFTJ is highly variable and has both deceptive and suppressive effects. To this end, both simulated and measured DFTJ data will be used in this paper for the jamming recognition analysis.

d) Interrupted Sampling and Repeating Jamming (ISRJ): ISRJ [46] uses a time-sharing forwarding system, *i.e.*, the jammer intermittently samples and then sequentially forwards radar signals, and the superposition of pulse compression results of these forwarding segments is capable of generating a large number of false targets. By adjusting the jammer transmitting and receiving parameters, the number and magnitude of the false targets can be rapidly changed, posing a serious threat to the radar system. Its time domain expression is

$$J_{ISRJ}(t) = \sum_{m=1}^{M} \sum_{n=0}^{N} rect\left(\frac{t - (nM + n + m)\,T_\omega}{T_\omega}\right) S\,(t - t_0 - mT_\omega) \tag{5}$$

where N is the number of jamming slices, T_ω and M represent the width of the slices and the number of forwarding.

e) Smart Noise Jamming (SNJ): SNJ [47] is a jamming signal generated by modulating intercepted radar signals with noise, which combines the effects of suppressive jamming and deceptive jamming. In this paper, we consider the basic amplitude modulated SNJ, in which Gaussian white noise is multiplied with the target echo signal and produces a large jamming bandwidth. The time-domain expression of SNJ is

$$J_{SNJ}(t) = n(t) \cdot S(t - t_0 - \tau_0) \tag{6}$$

B. Dataset construction and allocation for semi-supervised recognition tasks

This paper employs the LFM signal [48], which is widely used in pulse compression radar for its large time-bandwidth product to obtain high range resolution, as the radar transmit signal. The dataset S_t is composed of eight classes simulated jamming (DDJ, DFTJ, ISRJ, SNJ, BJ, DFTJ+SNJ, ISRJ+DDJ, SNJ+DDJ) and two measured jamming (BJ and DFTJ). The process of constructing the dataset is shown in Fig. 1. to

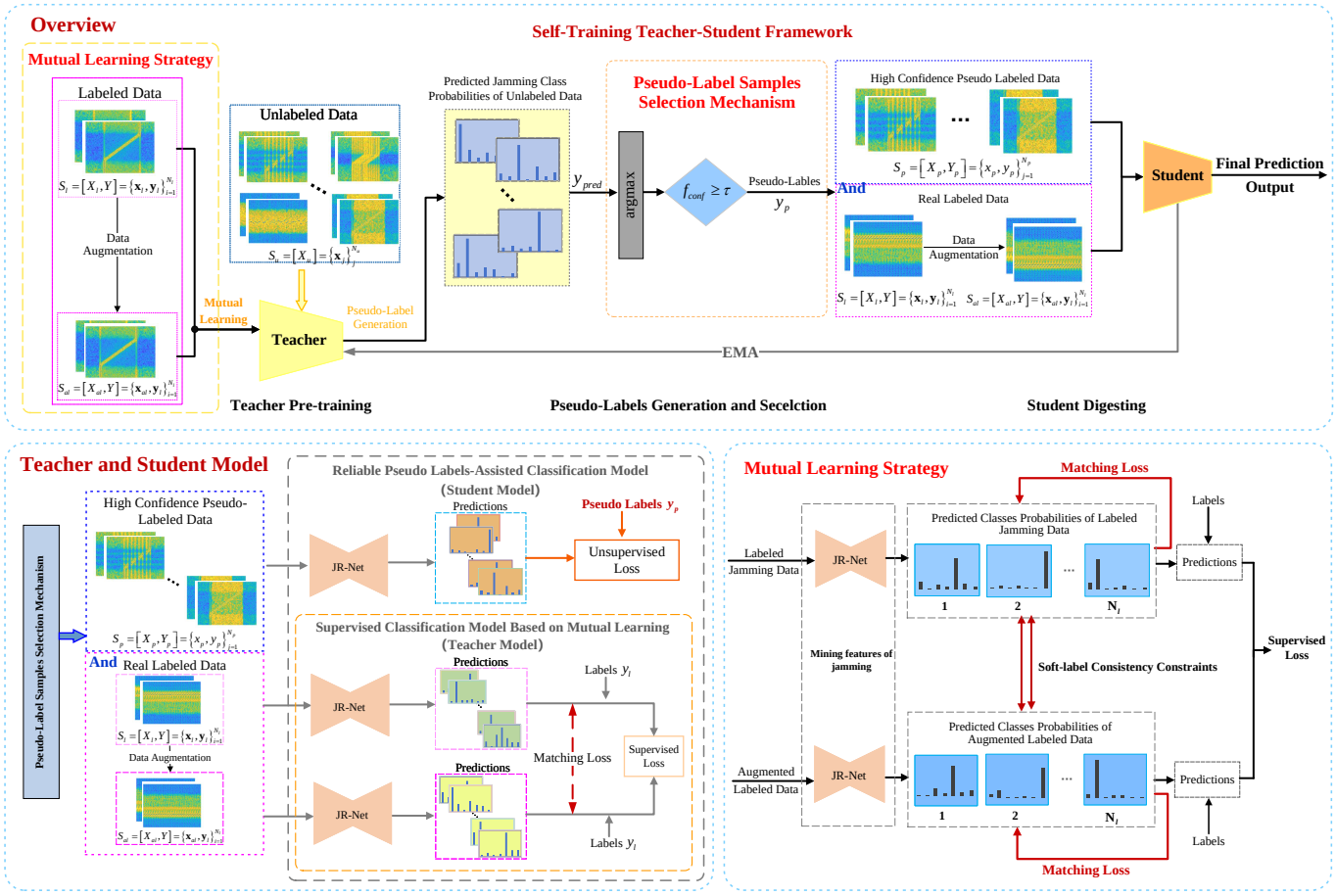

Fig. 2. Framework of the proposed SSJR-Net.

obtain the time-frequency data, short-time Fourier transform (STFT) [49] is performed on time-domain samples and its transformation can be formulated as

$$STFT_s(t,f) = \int_{-\infty}^{+\infty} s(\kappa)h^*(\kappa - t)exp(-j2\pi f\kappa)d\tau \tag{7}$$

where κ is the center of the window function $h^*(\kappa - t)$ in the time domain, * denotes the conjugate function, and $STFT(t,f)$ is a complex function.

Then, the real (R) and imaginary (I) parts of the jamming time-frequency matrix are extracted and fused to form the time-frequency dataset $I^S = \{I_R, I_I\}$. It is further divided into a very small-scale training set S_l and a large-scale testing set S_u. The training set containing N_l samples of the complex data matrix with class labels and N_u samples of the complex data matrix without labels, and can be expressed as follows

$$D_{train} = S_l \cup S_u = \{\mathbf{x}_l, \mathbf{y}\}_i^{N_l} \cup \{\mathbf{x}_u\}_j^{N_u} \tag{8}$$

and the testing set containing N_u samples of the complex data matrix without labels is expressed as $D_{test} = S_u = \{\mathbf{x}_u\}_j^{N_u}$, where $\mathbf{x}_l$ and $\mathbf{x}_u$ are both from the image set I^S , and $\mathbf{y}$ denotes the label corresponding to $\mathbf{x}_l$. In this way, the dataset obtained as above will be taken as input for network training and testing accordingly.

IV. Semi-supervised Jamming Recognition Network (SSJR-Net)

This paper proposes a novel perspective for accurate radar active jamming recognition under extreme scarcity of labeled data. It achieves robust and accurate recognition with few labeled data through self-training and semi-supervised learning. This section begins with a clear definition of semi-supervised radar active jamming recognition. Next, the overview of the proposed self-training teacher-student framework is introduced. Then, the mutual learning strategy and pseudo-labeled samples selection mechanism designed within the framework for improving the performance of the network are elaborated.

A. Problem Definition

The task of semi-supervised radar jamming recognition is formulated as follows. A dataset I^S is constructed for the training, which contains few labeled data and large amounts of unlabeled data. $S_l = [X_l, Y] = \{\mathbf{x}_l, \mathbf{y}\}_i^{N_l}$ denote N_l labeled jamming samples and $S_u = [X_u] = \{\mathbf{x}_u\}_j^{N_u}$ denote N_u unlabeled samples, where $\mathbf{x}_l$ and $\mathbf{x}_u$ represent the time-frequency matrix of jamming and $\mathbf{y}$ is the corresponding class label vector. The proposed method aims to achieve semi-supervised jamming recognition by exploiting a large amount of unlabeled data ($N_u \gg N_l$) to yield an improved recognition network with performance comparable to that of network trained using fully labeled dataset.

B. Self-Training Teacher-Student Framework

Due to the difficulty and complexity of radar jamming signal recognition training given a very small set of labeled data, a self-training teacher-student framework is introduced to achieve semi-supervised jamming recognition, and its overview is presented as overview in Fig. 2.

As illustrated in Fig. 2, the designed framework is made up of three parts: i) Training supervised classification model on a set of labeled data via mutual learning strategy (serves as the teacher model) and updating the parameters with exponential moving average (EMA) parameters; ii) Effectively employ the knowledge learned: pseudo-labels are generated for a large amount of unlabeled data by the teacher model to boost the learning of unlabeled data. Then, high-quality pseudo-labeled samples are selected based on the pseudo-label selection mechanism and added to training set; iii) Training the reliable pseudo-labels-assisted classification model (served as the student model) with both real labeled data and high-quality pseudo-labeled data based on the established objective function, and then keep training iteratively until robust and stable recognition results are obtained. Note that, since our method aims to design a semi-supervised framework for few-shot jamming recognition, thus improving the performance of the baseline. Therefore, the jamming recognition network (JR-Net) [29] is utilized as our baseline recognition network in both teacher and student model. With the support of the proposed method, a highly accurate and robust jamming recognition network without relying on extensive labeled data is achieved.

C. Mutual Learning Strategy (MLS)

To increase the diversity of the training data and reduce the risk of overfitting, the labeled data S_l was first processed using standard data augmentation including random flipping and rotation. With augmented labeled data $S_{al} = [X_{al}, Y] = \{\mathbf{x}_{al}, \mathbf{y}\}_i^{N_l}$ and original labeled data S_l, a mutual learning strategy (MLS) is proposed to improve the recognition accuracy and stability performance through collaborative training between the two labeled data sets, which is illustrated in Fig. 2. Specifically, the mutual learning strategy is able to learn more robust representations and thus improve the performance of the model by allowing two JR-Nets to learn from each other during the training process. The probability of class c for sample $\mathbf{x}_i$ predicted by the teacher model $\mathcal{T}$ is computed as

$$p^c(\mathbf{x}_i) = \frac{exp(z^c(\mathbf{x}_i))}{\sum_{c=1}^{C} exp(z^c(\mathbf{x}_i))} \tag{9}$$

where the logit z^c is the output of the "Softmax" layer in the teacher model $\mathcal{T}$, and C refers to the total number of jamming types in the constructed dataset.

As shown in Fig. 2, not only the loss between all labeled data and their true class labels, but also the matching loss between the predictions of the two labeled datasets are jointly used to constrain the process of training and thus enhance the robustness of the model. The loss between all labeled samples and their true class labels is defined as the cross-entropy loss which is computed as the inner product of one-hot truth label and the predicted probability,

$$\begin{aligned} L_{CE-l} &= -\frac{1}{N_l}\sum_{i=1}^{N_l}\sum_{c=1}^{C} I(\mathbf{y}_i, c)\, log\left(p_{\mathcal{T}}^c(\mathbf{x}_i)\right), \mathbf{x}_i \in \mathbf{x}_l \\ L_{CE-al} &= -\frac{1}{N_l}\sum_{i=1}^{N_l}\sum_{c=1}^{C} I(\mathbf{y}_i, c)\, log\left(p_{\mathcal{T}}^c(\mathbf{x}_i)\right), \mathbf{x}_i \in \mathbf{x}_{al} \end{aligned} \tag{10}$$

where $\mathbf{x}_l$ and $\mathbf{x}_{al}$ denote the labeled data and the augmented labeled data, respectively. And the indicator function $I(\cdot)$ is defined as

$$I(y_i, c) = \begin{cases} 1, \ if \ y_i = c \\ 0, \ otherwise \end{cases} \tag{11}$$

The matching loss $\mathcal{L}_{TM}$ between the prediction of labeled data and augmented labeled data in the teacher model is measured by L2 loss, which is expressed as follow

$$\mathcal{L}_{TM} = \frac{1}{N_l}\sum_{i=1}^{N_l}\sum_{c=1}^{C}\left\|p_{al}^c - p_l^c\right\|^2 \tag{12}$$

where p_{al} and p_l denote the predictions for augmented labeled data and labeled data, respectively. Thereby, mutual learning enforces consistency between JR-Nets, encouraging both to make similar predictions for the labeled samples and the augmented labeled samples, which leads to more stable and accurate recognition, especially in the case of extremely scarce labels.

Based on the mutual learning strategy, the supervised classification model can be trained through the loss function $L_{\mathcal{T}}$

$$L_{\mathcal{T}} = L_{CE-l} + L_{CE-al} + \alpha_{TM}\mathcal{L}_{TM} \tag{13}$$

where L_{CE-l} and L_{CE-al} denote the cross-entropy loss for the labeled data and the augmented labeled data, respectively. And parameter α_{TM} controls the weight of the matching loss in $L_{\mathcal{T}}$.

In this way, the supervised classification model based on mutual learning strategy is served as the teacher model and is capable of learning both the mapping between the features of the jamming signal and its true class labels, as well as recognizing distinctions and connections between different jamming classes, so the recognition performance of the model is effectively improved.

It is known that averaging model weights throughout the training process tends to improve model accuracy compared to relying solely on the final weights. Accordingly, we adopt the exponential moving average (EMA)-Teacher in our framework, which means that the weights of the teacher model are updated using a weighted average of its previous weights and the current weights of the student model. The teacher model weight is computed as:

$$\theta_{\mathcal{T}} \leftarrow \lambda\theta_{\mathcal{T}} + (1-\lambda)\,\theta_{\mathcal{S}} \tag{14}$$

where λ is a smoothing coefficient, which controls how much weight is given to the teacher's previous weights vs the student's current weights. $\theta_{\mathcal{T}}$ and $\theta_{\mathcal{S}}$ are the parameters of the teacher model and the student model, respectively. In this way, the teacher model updates the weights as EMA weights, allowing the model to be more stable and robust, thus providing a better guide for the student model.

Algorithm 1: Training of SSJR-Net.

input : Labeled training set $S_l = [X_l, Y] = \{\mathbf{x}_l, \mathbf{y}\}_i^{N_l}$; Unlabeled training set $S_u = [X_u] = \{\mathbf{x}_u\}_j^{N_u}$; The weights α_p, α_{TM}, α_{SM} and the coefficient λ.
output: The trained jamming recognition model $\mathcal{S}$

1 Augment labeled data by random flipping or rotation;
2 Train a teacher model $\mathcal{T}$ with the original labeled data from S_l and augmented labeled data S_{al} through mutual learning strategy;
3 Generate pseudo-labels on unlabeled data from S_u using $\mathcal{T}$;
4 Screening all generated pseudo-labels to obtain high-confidence pseudo-labeled data S_p, and loading parameters for the teacher model into the student model;
5 Train the student model $\mathcal{S}$ using all the training data, both real labeled data S_l and pseudo-labeled data S_p;
6 Iterative training: Calculate the loss function with (20) and update the teacher model using EMA student parameters as (14), then go back to Step 3
7 **return** $\mathcal{S}$

D. Pseudo-Label Samples Selection Mechanism (PLSM)

As the overview of the network in in ① of Fig. 2 shows, given the trained teacher model $\mathcal{T}$, the corresponding pseudo-labels for unlabeled samples can be made available through the pseudo-label generation mechanism. Since unlabeled data has no true class labels as a reference to constrain the network's prediction, the ability to filter out reliable pseudo-labels as the reference aiding the training of the labeled data is a critical step in self-training. In this paper, a pseudo-label selection mechanism is designed aiming to select the high-quality pseudo-label-assisted labeled data to train the network.

In our pseudo-label selection mechanism, a confidence threshold is used to filter soft pseudo-labels, which can be expressed as

$$M(\mathbf{x}_u) = \begin{cases} 1, \ if \ f_{conf} \geq \tau \\ 0, \ otherwise \end{cases} \tag{15}$$

where $M(\mathbf{x}_u)$ is the metrics function, τ is a scalar hyperparameter denoting the threshold which we retain a pseudo-label, and the f_{conf} is presented as

$$f_{conf} = \max\left(p(\mathbf{x}_u)\right) \tag{16}$$

where $p(\mathbf{x}_u)$ denotes the predicted class probability produced by the model for input $\mathbf{x}_u$. This refers to only retaining pseudo-labels whose largest class probability of the prediction exceeds a pre-designed threshold. In this way, after pseudo-label selection, the pseudo-labeled samples $S_p = [X_p, Y_p] = \left\{\mathbf{x}_p, \mathbf{y}_p\right\}_j^{N_p}$ can be used to train the reliable pseudo-labels-assisted classification model (serves as the student model) along with the original real labeled data, and N_p denotes the number of unlabeled data involved in the training process of student model. The pseudo-label $\mathbf{y}_p$ corresponding to the selected unlabeled sample $\mathbf{x}_p$ can be expressed as

$$\mathbf{y}_p = M(\mathbf{x}_p) \cdot p_{\mathcal{T}}(\mathbf{x}_p), \mathbf{x}_p \in X_u \tag{17}$$

where $p_{\mathcal{T}}(\mathbf{x}_p)$ denotes the prediction of the teacher model for pseudo-labeled data $\mathbf{x}_p$.

The structure of the student model is presented in Fig. 2. The high quality pseudo-labeled data S_p, can then be combined with real labeled data S_l as input to the student model. However, when training the student model, different training strategies are used for real labeled data and pseudo-labeled data. For real labeled data, the training process is constrained with matching loss and the traditional supervised learning based on their actual class labels. While for the pseudo-labeled data, a kind of unsupervised training is achieved by calculating the loss with reference to their pseudo-label obtained by the teacher model and the PLSM.

The student model is trained with loss $L_{\mathcal{S}}$, which is a combination of three loss terms: a supervised loss $\mathcal{L}_r$, a matching loss $\mathcal{L}_{SM}$ and an unsupervised loss $\mathcal{L}_p$. Specifically, $\mathcal{L}_r$ is just the standard cross-entropy loss on labeled data (both original labeled data and augmented labeled data):

$$\mathcal{L}_r = -\frac{1}{N_l} \sum_{i=1}^{N_l} \sum_{c=1}^{C} I(\mathbf{y}_i, c) \, log\left(p_{\mathcal{S}}^c(\mathbf{x}_i)\right) \tag{18}$$

where $p_{\mathcal{S}}^c(\mathbf{x}_i)$, $\mathbf{x}_i \in \{\mathbf{x}_l, \mathbf{x}_{al}\}$ denote the predictions of student model for the labeled samples, and $I(\cdot)$ is an indicator function as given in (11). The matching loss $\mathcal{L}_{SM}$ between the prediction of labeled data and augmented labeled data in the student model is similar to the matching loss within the teacher model in (12).

And the unsupervised loss $\mathcal{L}_p$ is defined as the loss generated by pseudo-labeled samples, which can be expressed as

$$\mathcal{L}_p = M(\mathbf{x}_u) \cdot L_{CE}\left(p_{\mathcal{S}}(\mathbf{x}_u), \mathbf{y}_p\right) \tag{19}$$

where $p_{\mathcal{S}}(\mathbf{x}_u)$ denote the predictions of the student model for pseudo-labeled samples, L_{CE} represents the cross-entropy loss function. It is thus clear that this loss for unlabeled data $\mathbf{x}_u$ is capable of obtaining plausible solutions without the real labels as a reference.

The final training objective function for the student model on both the labeled and unlabeled data is represented as

$$L_{\mathcal{S}} = \mathcal{L}_r + \alpha_p \mathcal{L}_p + \alpha_{SM} \mathcal{L}_{SM} \tag{20}$$

where $\alpha_p, \alpha_{SM} > 0$ are the weights corresponding to unsupervised loss $\mathcal{L}_p$ and matching loss $\mathcal{L}_{SM}$, respectively.

The entire training procedure for the proposed SSJR-Net is summarized in Algorithm 1.

E. Implementation Details

In teacher model, the key is mutual learning strategy. Specifically, it comprises two weight-shared branches following the network architecture in [29]. One branch processes the original labeled data through a JR-Net to obtain the prediction p_l^c, while the other processes augmented labeled data via an identical JR-Net to yield predictions p_{al}^c. Then, the consistency between the p_l^c and p_{al}^c, is constrained by utilizing standard cross-entropy and an L2 loss. With the support of the mutual learning strategy, a reliable teacher model can be obtained to generate pseudo-labels for unlabeled data. Then, the generated pseudo-labels are further refined using the pseudo-label selection mechanism (PLSM) to obtain high-quality pseudo-labeled data. In teacher model, the benefit of using two JR-Nets is that

This article has been accepted for publication in IEEE Transactions on Aerospace and Electronic Systems. This is the author's version which has not been fully edited and content may change prior to final publication. Citation information: DOI 10.1109/TAES.2025.3578404

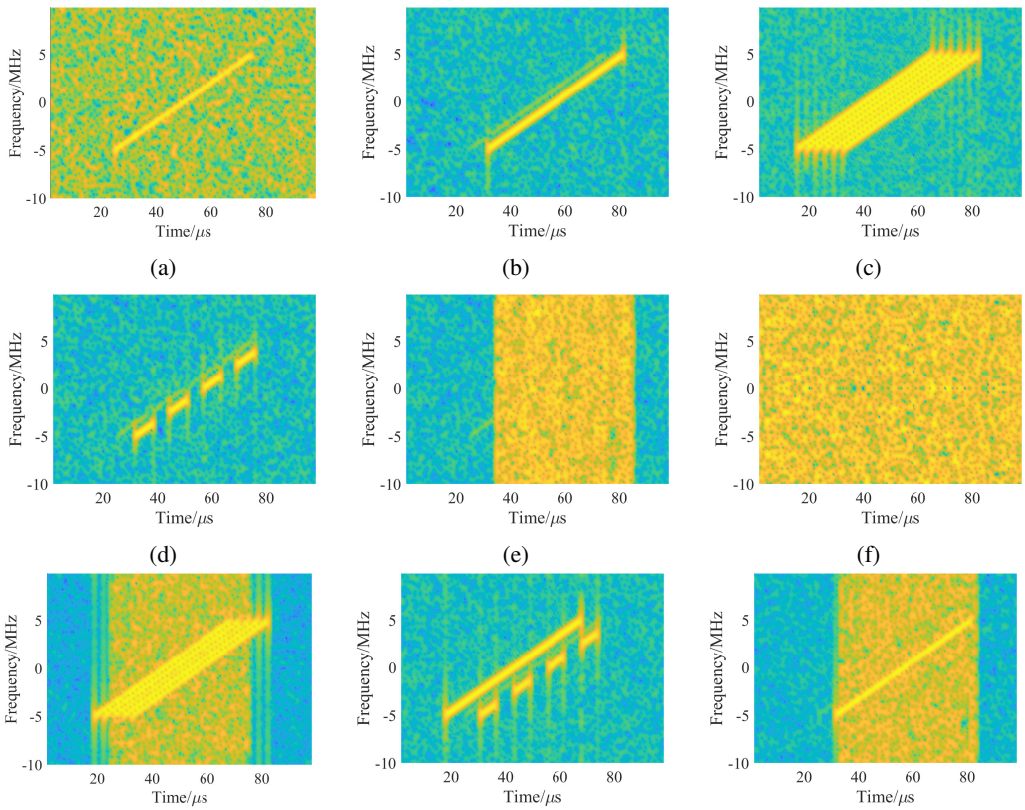

Fig. 3. Time-frequency spectrum of the simulated jamming signals in the dataset. (a) LFM (b) DDJ (c) DFTJ (d) ISRJ (e) SNJ (f) BJ (g) DFTJ+SNJ (h) ISRJ+DDJ (i) SNJ+DDJ

TABLE I
Parameter setting for the simulated signals

Signal	Parameters	Settings
LFM	Sampling frequency	20 MHz
	Time width	50 μs
	Bandwidth	10 MHz
	SNR	0 dB
DDJ	Delay in false target	1 ~ 11 μs
	JNR	10 ~ 30 dB
DFTJ	Delays in false targets	1 ~ 2.3 μs
	Number of false targets	3 ~ 7
	JNR	10 ~ 30 dB
ISRJ	Width of the slices	12.5 ~ 25 μs
	Number of forwarding	1 ~ 3
	JNR	10 ~ 30 dB
SNJ	Gaussian white noise	mean:0, variance: 1
	Others	Same as LFM
BJ	Bandwidth	15 ~ 20 MHz
	JNR	10 ~ 30 dB

the information of the jamming signals characterizing their time-frequency can be deeply mined, thus helping to boost the recognition accuracy and stability performance of the model.

In student model, it is trained in a semi-supervised manner. Specifically, it is firstly initialized with the teacher's weight parameters, and then jointly utilizes labeled data and high-quality pseudo-label data to train the third JR-Net. In particular, during the training by using the high-quality pseudo-label data, the predicted pseudo-labels from teacher model are served as the ground-truth to supervise the training of the model. In student model, the benefit of using the third JR-Nets is that the information of the unlabeled data can be effectively mined and utilized to advance the jamming recognition performance while not disturbing the knowledge of the teacher model.

V. Experiments and Results

In this section, we first detail the parameters for the radar jamming signal dataset and the assignment of labeled and unlabeled data for the semi-supervised recognition task. Then, the experimental configurations and the performance evaluation indicators used in this paper are described. Existing radar active jamming recognition methods are then used in comparative experiments on the constucted dataset to validate the outstanding performance of our SSJR-Net. Finally, ablation experiments and discussions are provided to demonstrate the contribution of the components in the proposed method.

A. Datasets

The dataset constructed in Section III is used to analyze the performance of the proposed SSJR-Net for radar active jamming recognition. There are simulated and measured jamming samples in the dataset, including eight types simulated radar active jamming samples, two types measured jamming samples, and one type of non-jamming samples, with 500

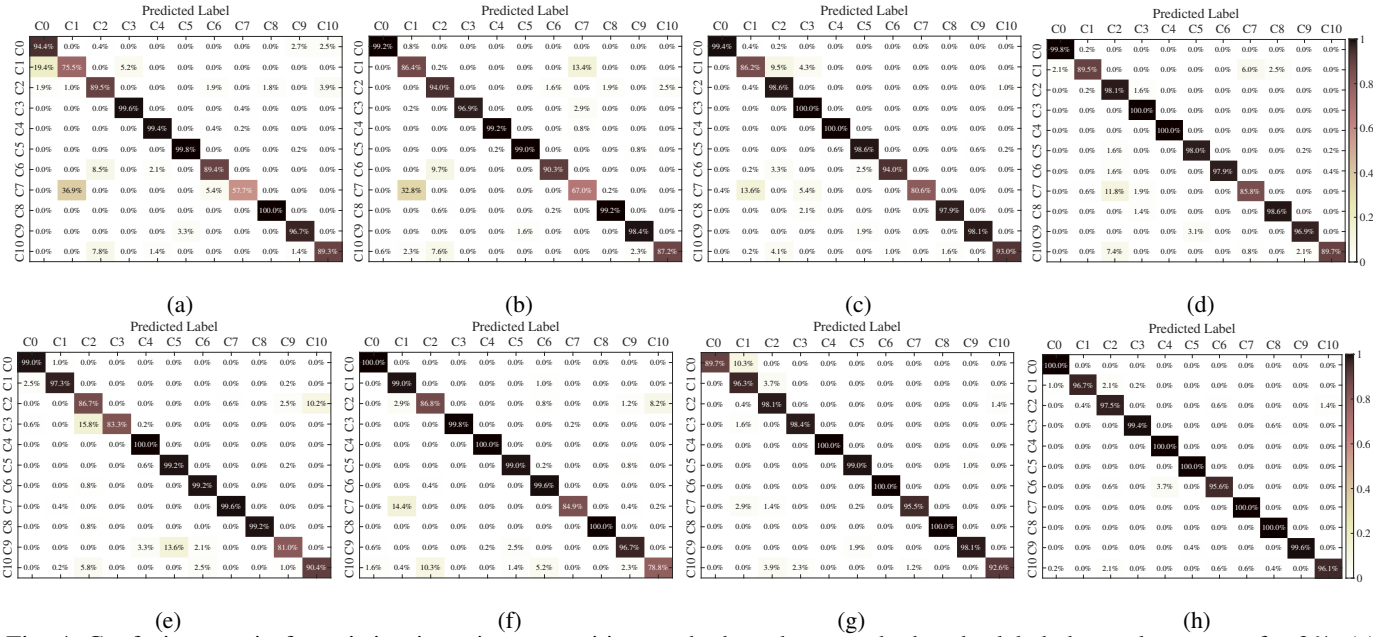

Fig. 4. Confusion matrix for existing jamming recognition methods and our method under labeled sample account for 3%. (a) 2D-CNN (b) WECNN-TL [28] (c) JR-TFSAD [29] (d) JR-ACAR [32] (e) SMTRNet [36] (f) BFE-ACGAN [38] (g) YBM [50] (h) SSJR-Net (Ours)

samples in each class. In addition, each simulated sample comprises a true target echo with an SNR of 0 dB. For each individual class of simulated jamming signals, their simulation parameters are shown in TABLE I. The composite jamming signals (DFTJ+SNJ, ISRJ+DDJ, SNJ+DDJ) are generated by combining the corresponding classes of radar jamming signals with different jamming-to-noise ratios (JNR) and different parameters. The generated time-domain jamming waveforms are used to produce time-frequency images by STFT transformation. Fig. 3 shows the time-frequency spectrum from the 9 types of simulated signals in the dataset (a randomly selected sample of each class). And the input images are resized to 256 × 128. In addition, to satisfy the setting of semi-supervised learning, we randomly sample 1%, 2%, 3%, 4% and 5% of radar jamming examples in the dataset to construct the labeled training set, and the remaining is used as the unlabeled training set and testing set.

B. Experimental Settings and Evaluation Metrics

Simulated data is generated with MATLAB 2020, and the DL experiments are implemented based on Pytorch framework, with training conducted on a server loaded with an RTX 3090 GPU. The initial learning rate is set to 2.0×10^{-4} and the ADAM algorithm [51] is used as the optimizer. The teacher model is pre-trained for 40 epochs, while the total number of training epochs is set to 140, with a batch size of 5. In addition, the jamming recognition network (JR-Net) presented in Fig. 2 follows a time-frequency self-attention model [29].

Moreover, to obtain more reliable conclusions, we use a set of evaluation metrics (including Precision [52], Recall [53], Micro-F1 [54], Overall Accuracy [55] Kappa [55]) to quantitatively measure the recognition performance of each method in the radar jamming recognition task to avoid one-sided or even erroneous conclusions that may be obtained by using only a single metric.

C. Performance Against Existing Recognition Methods

To validate the outstanding advantages of our SSJR-Net over existing methods in the few-shot radar jamming recognition task, 2D-CNN, WECNN-TL [28], JR-TFSAD [29], JR-ACAR [32], YOLO-based method (YBM) [50] and the semi-supervised learning methods SMTRNet [36], BFE-ACGAN [38] are used for comparison experiments. In these experiments, during the training process, the measured jamming data is merged with the corresponding simulated jamming data. During the testing stage, the measured and simulated data are predicted separately to evaluate the performance of the proposed method and the comparison methods exactly. And each result is obtained through five times independent testing.

The confusion matrix shown in Fig. 4 reflects the recognition performance of the comparison methods and our SSJR-Net for different jamming types with labeled samples accounting for 3% of the dataset. Each row represents the actual class of the jamming sample, and each column represents the predicted class. C0 ~ C10 represent Non-jamming, DDJ, DFTJ, ISRJ, SNJ, BJ, DFTJ+SNJ, ISRJ+DDJ, SNJ+DDJ, BJ (Measured) and DFTJ (Measured). From Fig. 4, compared to the sate-of-the-art jamming recognition methods, our SSJR-Net (Fig. 4 (f)) shows a significant improvement in recognition accuracy for most jamming types in the dataset, which demonstrates that the effective exploration of the latent value in unlabeled jamming data offers considerable benefits for few-shot radar jamming recognition tasks.

To verify the superiority of our SSJR-Net with even smaller samples, we conducted repeated experiments with 5 labeled samples for each jamming class. The experimental results of Overall Accuracy (OA), Kappa and testing time are presented

This article has been accepted for publication in IEEE Transactions on Aerospace and Electronic Systems. This is the author's version which has not been fully edited and content may change prior to final publication. Citation information: DOI 10.1109/TAES.2025.3578404

TABLE II
Results of the comparative experiment with 1% labeled data (5 labeled samples for each class)

Metric \ Method	2D-CNN	WECNN-TL [28]	JR-TFSAD [29]	JR-ACAR [32]	SMTRNet [36]	BFE-ACGAN [38]	YBM [50]	SSJR-Net (Ours)
OA	80.17±2.88	86.78±1.94	90.03±1.69	92.60±1.34	87.02±1.90	89.07±1.66	92.34±1.77	**96.35±0.67**
KAPPA	77.95±2.96	85.30±1.99	88.92±1.72	91.77±1.37	85.56±1.93	87.85±1.68	91.48±1.65	**95.94±0.70**
Testing time (s)	32.23±0.82	273.89±4.53	32.35±0.82	32.26±0.82	39.89±1.23	25.91±0.76	29.72±0.77	32.23±0.81

TABLE III
Recall (values±standard deviation) for several methods with 1% labeled data (5 labeled samples for each class)

Class	Recall (%)							
	2D-CNN	WECNN-TL [28]	JR-TFSAD [29]	JR-ACAR [32]	SMTRNet [36]	BFE-ACGAN [38]	YBM [50]	SSJR-Net (Ours)
Non-jamming	90.71±1.93	99.60±0.40	96.97±1.21	95.96±1.21	99.80±0.20	98.79±0.81	80.61±3.72	**100.00±0.00**
DDJ	53.33±5.19	61.01±4.78	63.84±4.18	71.92±3.80	86.46±2.23	**87.88±1.64**	87.87±2.61	78.59±3.03
DFTJ	50.71±5.83	74.14±3.90	95.96±1.60	98.38±0.97	53.33±4.65	77.78±3.81	96.36±1.21	**99.80±0.20**
ISRJ	77.37±4.12	81.82±2.55	79.39±3.17	98.79±0.81	71.11±3.66	**98.99±0.40**	85.86±2.94	94.14±0.81
SNJ	**100.00±0.00**	96.97±1.37	99.60±0.40	**100.00±0.00**	**100.00±0.00**	**100.00±0.00**	**100.00±0.00**	**100.00±0.00**
BJ	97.98±0.95	97.78±0.93	97.98±1.00	98.38±1.01	97.37±1.46	97.17±1.62	98.99±0.55	**100.00±0.00**
DFTJ+SNJ	76.77±3.49	98.99±0.60	97.58±0.87	98.59±0.59	99.80±0.20	99.60±0.40	**100.00±0.00**	98.79±0.40
ISRJ+DDJ	57.58±5.66	62.02±4.76	75.15±3.86	71.72±3.85	**96.97±1.85**	80.20±3.67	84.85±3.36	93.94±1.41
SNJ+DDJ	95.16±1.00	98.79±0.31	**100.00±0.00**	**100.00±0.00**	96.57±0.78	**100.00±0.00**	**100.00±0.00**	**100.00±0.00**
BJ (Measured)	95.56±1.72	96.56±1.20	96.77±1.04	97.58±1.01	65.86±4.41	87.68±1.89	96.16±1.52	**99.60±0.20**
DFTJ (Measured)	86.67±2.40	86.87±2.11	87.07±1.58	86.92±1.56	89.90±2.50	51.72±4.32	85.05±3.41	**94.95±1.21**
Average	80.16±2.90	86.77±1.96	90.17±1.70	92.57±1.35	87.01±1.92	89.14±1.67	92.34±1.76	**96.34±0.66**

TABLE IV
Precision(values±standard deviation) for several methods with 1% labeled data (5 labeled samples for each class)

Class	Precision (%)							
	2D-CNN	WECNN-TL [28]	JR-TFSAD [29]	JR-ACAR [32]	SMTRNet [36]	BFE-ACGAN [38]	YBM [50]	SSJR-Net (Ours)
Non-jamming	99.34±0.66	**100.00±0.00**	83.48±2.00	85.13±2.17	81.52±2.81	87.63±2.12	**100.00±0.00**	97.06±0.95
DDJ	80.73±3.15	58.30±5.11	81.23±2.61	73.55±4.31	**96.40±1.31**	78.10±3.03	67.76±5.43	96.05±1.73
DFTJ	69.72±4.24	**99.73±0.27**	63.84±3.95	84.26±2.49	65.18±4.63	80.38±2.38	77.43±4.25	77.80±2.89
ISRJ	96.23±1.41	**100.00±0.00**	93.79±1.95	**100.00±0.00**	**100.00±0.00**	**100.00±0.00**	95.08±1.88	97.49±0.86
SNJ	95.19±0.89	98.16±0.85	99.60±0.25	99.00±0.57	92.87±1.32	96.49±1.26	99.80±0.11	**100.00±0.00**
BJ	95.66±1.72	96.61±1.75	96.42±1.78	97.60±1.46	92.34±1.75	94.13±1.29	93.69±2.16	**99.60±0.21**
DFTJ+SNJ	60.80±5.23	96.46±1.73	94.71±1.70	88.41±2.00	81.65±2.80	91.46±1.58	**98.80±0.35**	98.39±0.95
ISRJ+DDJ	87.42±2.87	54.53±5.38	96.37±1.67	98.07±0.82	**100.00±0.00**	97.78±0.97	98.13±1.10	99.15±0.34
SNJ+DDJ	96.71±1.90	88.27±1.96	**100.00±0.00**	99.60±0.07	99.80±0.20	**100.00±0.00**	**100.00±0.00**	**100.00±0.00**
BJ (Measured)	94.41±2.04	86.28±2.69	98.36±1.32	98.98±0.15	86.93±2.28	76.68±3.25	99.17±0.11	**100.00±0.00**
DFTJ (Measured)	45.54±5.63	87.40±2.38	97.51±1.60	98.18±0.96	69.10±4.43	77.34±3.35	**100.00±0.00**	99.79±0.08
Average	83.80±2.96	87.79±2.01	91.52±1.71	92.98±1.37	87.80±1.95	90.78±1.73	93.67±1.59	**96.85±0.74**

in TABLE II, where testing time testing time denotes the total time required to recognize all samples in the testing set. As shown in TABLE II, compared to the existing fully-supervised and semi-supervised recognition methods, our SSJR-Net has a significant performance improvement in the recognition accuracy without sacrificing the testing time. This indicates that the proposed SSJR-Net performs satisfactorily both in terms of recognition accuracy and stability.

Then, the results of Recall, Precision, and Micro-F1 using comparison methods and our SSJR-Net with 5 labeled samples as the training set for jamming recognition are presented in TABLE III to V, respectively. Among them, the bold font indicates the maximum value recognized for each type of jamming. As seen in TABLE III to V, the proposed SSJR-Net shows significant improvements in all three metrics. Specifically, SSJR-Net achieves improvements of 3.77%-16.18%, 3.18%-13.05% and 3.86%-15.82% in average Recall, Precision, and Micro-F1 over the existing methods. Furthermore, compared to existing fully supervised and semi-supervised recognition methods, our semi-supervised method demon-

This article has been accepted for publication in IEEE Transactions on Aerospace and Electronic Systems. This is the author's version which has not been fully edited and content may change prior to final publication. Citation information: DOI 10.1109/TAES.2025.3578404

TABLE V
Micro-F1(values±standard deviation) for several methods with 1% labeled data (5 labeled samples for each class)

Class	Micro-F1 (%)							
	2D-CNN	WECNN-TL [28]	JR-TFSAD [29]	JR-ACAR [32]	SMTRNet [36]	BFE-ACGAN [38]	YBM [50]	SSJR-Net (Ours)
Non-jamming	94.83±1.40	**99.80±0.06**	89.72±1.57	90.22±1.34	89.74±2.03	92.88±1.36	89.26±2.66	98.51±0.50
DDJ	64.23±4.78	59.62±4.90	71.49±3.71	72.73±3.89	**91.16±1.59**	82.70±2.51	76.52±4.51	86.44±2.11
DFTJ	58.71±5.15	85.05±2.11	76.67±3.45	**90.77±1.75**	58.67±4.55	79.06±3.00	85.87±2.95	87.43±2.03
ISRJ	85.78±2.92	90.00±1.63	86.00±2.28	99.39±0.61	83.11±1.50	**99.49±0.21**	90.23±1.53	95.79±0.83
SNJ	97.54±1.02	97.56±0.95	99.60±0.12	99.50±0.24	96.30±0.86	98.21±0.91	99.90±0.09	**100.00±0.00**
BJ	96.81±1.29	97.19±1.01	97.19±1.12	97.99±1.06	94.79±1.58	95.63±1.45	96.55±1.37	**99.80±0.09**
DFTJ+SNJ	67.86±4.23	**97.71±0.94**	96.12±1.38	93.22±1.21	89.82±1.72	95.36±0.93	99.40±0.31	98.59±0.88
ISRJ+DDJ	69.43±4.11	58.03±5.02	84.45±2.46	82.85±2.80	**98.46±0.93**	88.12±1.56	91.01±1.88	96.47±0.91
SNJ+DDJ	95.93±1.15	93.23±1.49	**100.00±0.00**	99.80±0.10	98.15±0.75	**100.00±0.00**	**100.00±0.00**	**100.00±0.00**
BJ (Measured)	94.98±1.62	91.13±1.55	97.56±1.17	98.27±0.61	74.94±3.20	81.81±2.78	97.64±1.29	**99.80±0.10**
DFTJ (Measured)	59.71±5.05	87.13±2.27	92.00±1.49	92.21±1.40	78.14±3.24	61.99±4.35	91.92±2.06	**97.31±0.99**
Average	80.53±2.92	86.95±1.96	89.56±1.70	92.45±1.35	86.92±1.94	88.74±1.71	92.49±1.70	**96.35±0.76**

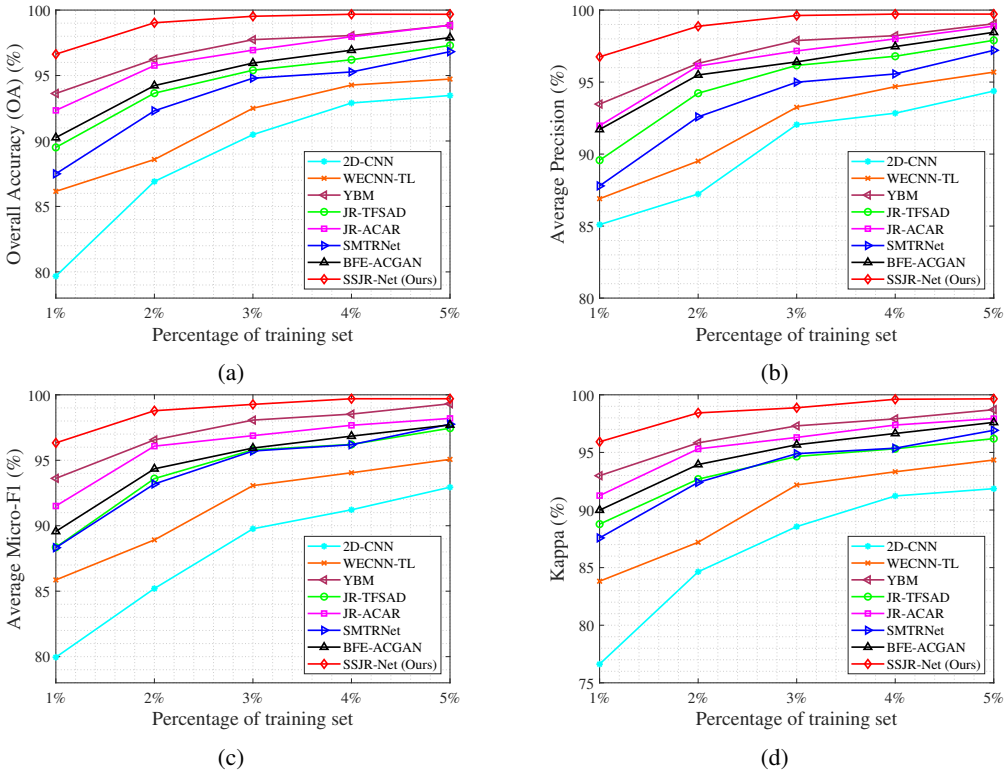

Fig. 5. Variation curve of performance indicators with the size of labeled data. (a) OA (b) Precision (c) Micro-F1 (d) Kappa

strates the highest stability, showing the least fluctuation in the results. These results demonstrate that exploiting the implicit information from the labeled data and transferring the knowledge to further extract the information implicit in unlabeled data provides an effective aid to network training resulting in further improvement in the recognition performance of the model. Furthermore, the above experimental results indicate that the proposed method can achieve accurate and reliable radar active jamming recognition even with extremely small number of labeled training samples.

In addition, several independent experiments were conducted on the existing methods and our SSJR-Net with labeled data accounting for 1%, 2%, 3%, 4% and 5% of the constructed dataset, respectively. Fig. 5 illustrates the average results of five experiments. Since the values of the average Recall and OA are shown to be equal through the experimental results, the curves of OA, Kappa, average Precision and Micro-F1 vs the size of labeled data are presented. From Fig. 5, it is clear that SSJR-Net achieves superior recognition performance compared to the existing fully-supervised and the semi-supervised recognition methods when the labeled data are of the same size. Moreover, as the labeled data size decreases, the advantage of SSJR-Net becomes increasingly apparent. This can be attributed to the integration of reliable pseudo-labeled

This article has been accepted for publication in IEEE Transactions on Aerospace and Electronic Systems. This is the author's version which has not been fully edited and content may change prior to final publication. Citation information: DOI 10.1109/TAES.2025.3578404

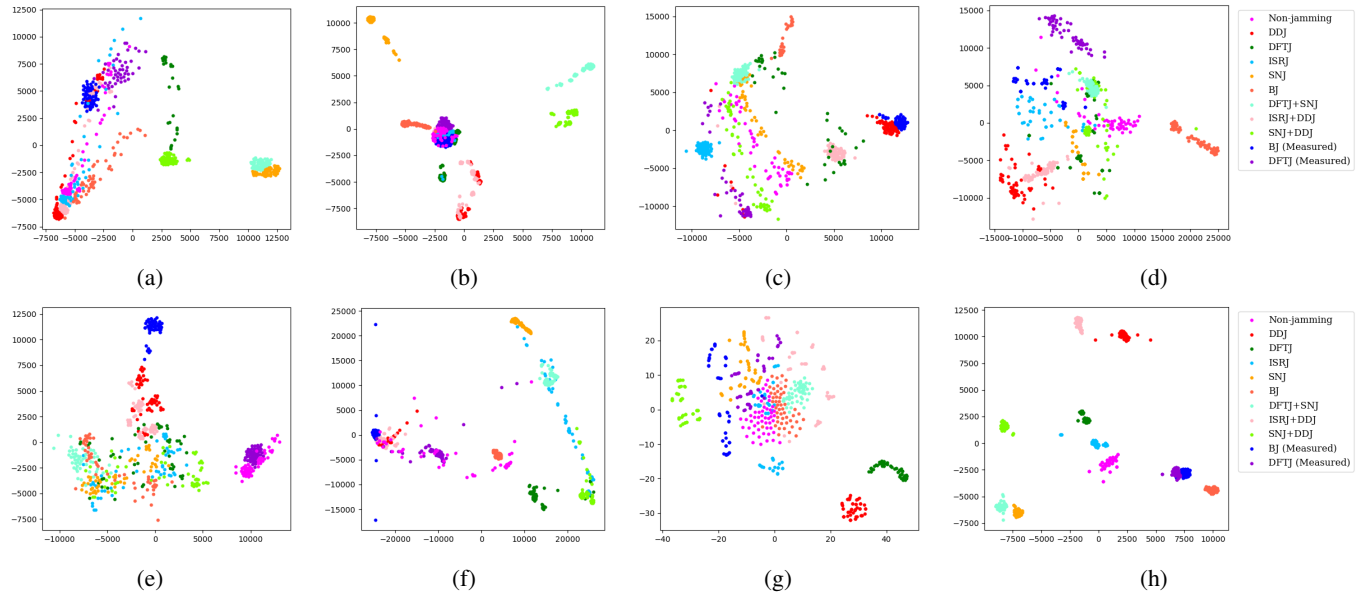

Fig. 6. t-SNE visualization: Feature representation performance of the existing jamming recognition methods and the proposed SSJR-Net, each color denotes one class (a) 2D-CNN (b) WECNN-TL [28] (c) JR-TFSAD [29] (d) JR-ACAR [32] (e) SMTRNet [36] (f) BFE-ACGAN [38] (g) YBM [50] (h) SSJR-Net (Ours)

TABLE VI
Ablation Study of the Contribution of Each Mechanism/Components

Structure			Evaluation Metrics					
ST	MLS	PLSM	OA (%)	Kappa (%)	Average Precision (%)	Average Micro-F1 (%)	Training time (s)	Testing time (s)
×	×	×	90.54±1.68	89.49±1.52	91.78±1.66	90.53±1.65	225.28	32.21
✓	×	×	92.75±1.37	91.93±1.42	93.42±1.51	92.50±1.47	239.88	32.23
✓	✓	×	94.14±1.15	93.45±1.13	94.76±1.20	93.93±1.15	261.45	32.24
✓	✓	✓	96.34±0.75	95.94±0.81	96.78±0.75	96.33±0.77	271.93	32.24

data and training by means of semi-supervised learning, which boosts the network effectively learn the internal features of the jamming time-frequency data. The results also reveal that recognition performance declines as the labeled data size reduced. However, even with only 1% of labeled data, our SSJR-Net still achieves satisfactory recognition performance.

D. Quality Assessment of Feature Expression

To further validate the superior feature representation capabilities of our SSJR-Net, we conducted the following experiments. In these experiments, we employ the same dataset described in Section V-A, with 5 labeled samples per class for model training. The t-SNE is exploited to create 2D visualizations of the embeddings from the testing set, and results is presented in Fig. 6. The features displayed here for each network are extracted prior to the final layer during testing.

As shown in Fig. 6, for 2D-CNN and WECNN-TL, the features of some jamming classes are separable from each other, but the clustering centers of most of the classes are not distinctly separated. For YOLO-based method [50], the features of each class do not form clusters, but are distributed in a mixed way, which makes the probability of misclassification between the different classes increase dramatically. The features extracted by JR-TFSAD between classes are separated but lack clear clustering within each class. Furthermore, the feature centers of the categories extracted by two semi-supervised methods SMTRNet [36] and BFE-ACGAN [38] are also clustered together. In contrast, as shown in Fig. 6 (f), SSJR-Net displays distinct feature distributions across most classes with clear class boundaries. Especially for the classes DDJ and DDJ+ISRJ, compared to other methods, the features extracted by our SSJR-Net are highly discriminative and their clustering centers are very far away from each other. This phenomenon vividly illustrates that the proposed SSJR-Net effectively improves the feature representation of the network through unlabeled data-assisted training in a self-training semi-supervised manner.

E. Ablation Studies

This section presents ablation experiments to evaluate the effectiveness of the proposed key components. The experiments are performed on the dataset constructed in Section III with 1% labeled radar jamming samples (5 labeled samples for each class). The results of the ablation experiment for the self-

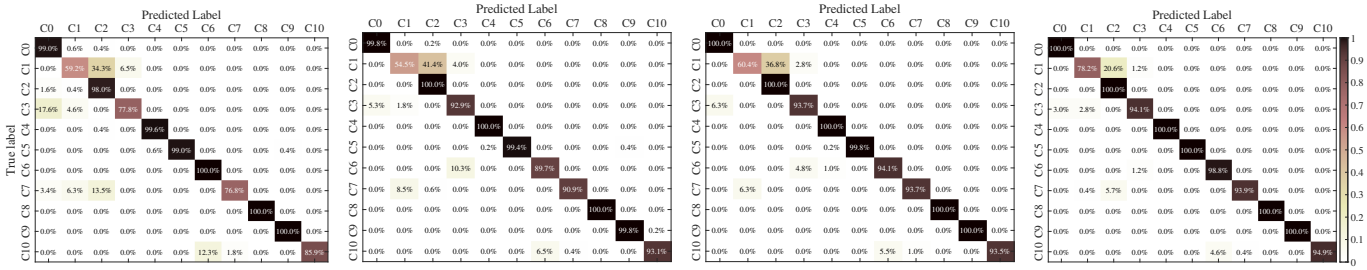

(a) (b) (c) (d)

Fig. 7. Confusion matrix for the ablation experiments. (a) Only Teacher Model (b) Teacher Model+ST (c) Teacher Model+ST+MLS (d) Teacher Model+ST+ML+PLSM (The proposed SSJR-Net)

TABLE VII
Comparison experimental results with 5% labeled training data

Method	Labeled training data	OA (%)	Kappa (%)	Average Precision (%)	Average Micro-F1 (%)
WECNN-TL [28]	5%	94.03±1.27	93.36±1.29	94.49±1.29	94.05±1.28
JR-TFSAD [29]		97.10±0.78	96.21±0.77	97.91±0.81	97.13±0.79
JR-ACAR [32]		98.16±0.61	97.97±0.62	98.29±0.64	98.17±0.62
SSJR-Net (Ours)		**99.69±0.12**	**99.66±0.13**	**99.70±0.13**	**99.69±0.12**

training framework are shown in TABLE VI. Specifically, '×' and '✓' indicate the absence or presence of the corresponding component within the method, respectively. Except for the above evaluation indicators, the training time and testing time for the ablation of each component are presented to demonstrate their impact on the time effectiveness of the method. Moreover, the confusion matrices obtained by ablating each key component are shown in Fig. 7 to further demonstrate the effectiveness of the proposed method.

a) Effectiveness of Self-Training (ST): From the first and second rows of TABLE VI, it can be seen that the proposed self-training teacher-student framework significantly improves the model's recognition accuracy of radar active jamming when there are few labeled data, with OA, Kappa average Precision and average Micro-F1 improved by 4.95%, 5.36%, 3.04% and 4.12%, respectively. This indicates that self-training effectively improves the feature extraction and recognition ability of the network for radar active jamming without utilizing additional labeled data.

b) Effectiveness of mutual learning strategy (MLS): The second and third rows of TABLE VI show the results of the ablation experiments on the proposed MLS. From Fig. 7 (b) and Fig. 7 (c) as well as the results in TABLE VI, it can be deduce that the MLS makes effective utilization of the labeled data through constraints of the matching loss in the interactive learning between prediction of the original labeled data and the augmented data, thus improving the quality of the model's prediction for the jamming class. Furthermore, with the MLS, the variance of the model on the testing set has been significantly reduced, it corroborates that MLS appears to be helping to find a more robust minimum that generalizes better to test data.

c) Effectiveness of PLSM: From Fig. 7 (c) and Fig. 7 (d) and the results in TABLE VI, it is clear that with the pseudo-labeled samples selection mechanism, the recognition performance of the network for all types of jamming in the dataset had improved, especially for the DDJ (C1) and DFTJ+SNJ (C5) among them, the recognition accuracy has improved significantly. Furthermore, although the training time is slightly increased, it is obvious that the proposed PLSM not only improves the recognition accuracy of the model, but more importantly, the variance of the model on the testing set is significantly reduced. This suggests that low-confidence pseudo-labels are eliminated through the PLSM, and high-quality pseudo-labeled samples are capable of further facilitating the feature extraction as well as improving the robustness and stability of the recognition network.

In summary, the effectiveness of each proposed key components in the jamming recognition task has been verified by ablation experiments, and these findings also explain why our proposed semi-supervised recognition network improves the recognition performance under extremely limited number of labeled data.

F. Discussions

a) Recognition performance with general few-shot setting (5% labeled training data): TABLE VII presents a comparative performance of state-of-the-art few-shot jamming recognition methods and the proposed method with 5% labeled training data on the dataset described in Section V-A. From the results, it can be seen that the performance of the proposed method is significantly superior to these methods under the few-shot setting described in these references, which is attributed to the complete exploration of valuable information contained in the unlabeled data.

b) Recognition performance with varying size of the dataset: To investigate the effect of the labeled samples' number on performance, we expanded the size of the dataset to retrain the network of different methods. Specifically, the

TABLE VIII
Comparison of recognition performance with different numbers of training samples

Method	Labeled training data	OA (%)	Kappa (%)	Average Precision (%)	Average Micro-F1 (%)
JR-TFSAD [29]	5 shots per class	90.03±1.69	88.92±1.72	91.52±1.71	89.56±1.70
JR-ACAR [32]		92.60±1.34	91.77±1.37	92.98±1.37	92.45±1.35
SSJR-Net (Ours)		**96.35±0.75**	**95.94±0.81**	**96.85±0.74**	**96.35±0.76**
JR-TFSAD [29]	10 shots per class	93.16±1.13	92.19±1.15	93.74±1.12	93.11±1.14
JR-ACAR [32]		94.15±0.96	93.35±0.97	94.90±0.99	93.95±0.96
SSJR-Net (Ours)		**98.68±0.18**	**98.05±0.21**	**99.09±0.20**	**98.77±0.19**
JR-TFSAD [29]	20 shots per class	95.61±0.90	94.73±0.88	96.20±0.92	95.62±0.91
JR-ACAR [32]		96.75±0.68	95.80±0.66	97.03±0.72	96.76±0.69
SSJR-Net (Ours)		**99.19±0.14**	**99.08±0.14**	**99.19±0.15**	**99.18±0.14**

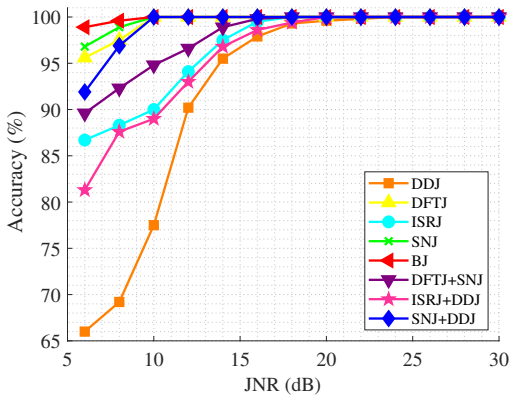

Fig. 8. Trend of recognition performance vs. JNR for the proposed SSJR-Net.

number of samples per class is increased to two and four times the original, reaching 1000 and 2000, respectively. Then experiments are conducted with 1% labeled data during training. The experimental results are shown in TABLE VIII. As shown in TABLE VIII, when the total dataset size increases and the number of training data for each class grows to 10 and 20, the proposed method still achieves the best performance, thus verifying the effectiveness of the proposed method.

c) Recognition performance with varying JNR: To explore the performance variation of the proposed method under different JNRs, it is tested with 100 samples of each jamming type at each JNR, and the variation of recognition accuracy is shown in Fig. 8. From Fig. 8, it can be seen that for DFTJ, SNJ, BJ, and SNJ+DDJ, the recognition accuracy remains nearly 100% over the JNR range of 10 to 30 dB. As the JNR increases, the recognition accuracy for these jamming types improves significantly, and when JNR exceeds 16 dB, the accuracy stabilizes above 98% for all simulated jamming types. These findings demonstrate that the proposed method can achieve reliable few-shot jamming recognition across a wide range of JNR conditions. Overall, although the labeled training samples are only 1% of the total dataset, the proposed method still shows satisfactory accuracy on the test set (the remaining 99% data of the total dataset). These results validate the effectiveness of the proposed semi-supervised method in enhancing jamming recognition performance in real-world scenarios with scarce labeled samples.

VI. Conclusions

In this paper, we proposed a novel SSJR-Net for few-shot radar active jamming recognition, which aims to alleviate the issue of insufficient labeled dataset and poor performance by leveraging on the unlabeled data. In the proposed self-training teacher-student framework, a mutual learning strategy and a pseudo-label samples selection mechanism are designed to enhance the performance for the semi-supervised radar jamming recognition. On the one hand, to effectively mine the recognition-related knowledge from labeled data and transfer such useful knowledge into the recognition of the unlabeled data, a mutual learning strategy by minimizing the matching loss is proposed. On the other hand, based on the generated pseudo-labels, a pseudo-labeled samples selection mechanism is proposed to filter high-quality pseudo-labeled samples through designed confidence threshold comparison module, thus effectively assisting in the training of the few-shot recognition network. By jointly using the two mentioned components in the self-training framework, our network allows for the learning of robust and discriminative features from both labeled and unlabeled data, and effectively reducing the reliance on labeled data for supervised learning. Extensive experiments on a dataset combining simulated and measured data show that our SSJR-Net outperforms state-of-the-art radar jamming recognition methods, achieving superior recognition accuracy, better stability, and comparable computational efficiency. More importantly, since the effective exploitation for unlabeled data and alleviating the reliance on extensive labeled datasets, the proposed method has high application value in complex battlefield environments.

References

[1] L. Zhang, G. Wang, Z. Qiao, H. Wang, and L. Sun, "Two-stage focusing algorithm for highly squinted synthetic aperture radar imaging," *IEEE Transactions on*

Geoscience and Remote Sensing, vol. 55, no. 10, pp. 5547–5562, 2017.

[2] Z. Yang, Z. Li, X. Yu, Q. Zhou, C. Huang, and J. Zhang, "Maximin design of wideband constant modulus waveform for distributed precision jamming," *IEEE Transactions on Signal Processing*, vol. 72, pp. 1316–1332, 2024.

[3] Y. Luo, Y.-a. Chen, Y.-x. Sun, and Q. Zhang, "Narrowband radar imaging and scaling for space targets," *IEEE Geoscience and Remote Sensing Letters*, vol. 14, no. 6, pp. 946–950, 2017.

[4] Y. He, T. Zhang, H. He, P. Zhang, and J. Yang, "Polarization anti-jamming interference analysis with pulse accumulation," *IEEE Transactions on Signal Processing*, vol. 70, pp. 4772–4787, 2022.

[5] J. Wei, Y. Li, R. Yang, E. Zhu, J. Ding, M. Ding, and P. Zhang, "A time domain filtering method based on intra-pulse joint inter-pulse coding to counter interrupted sampling repeater jamming in sar," *IEEE Transactions on Geoscience and Remote Sensing*, 2023.

[6] Y. Shi, X. Lu, Y. Niu, and Y. Li, "Efficient jamming identification in wireless communication: Using small sample data driven naive bayes classifier," *IEEE wireless communications letters*, vol. 10, no. 7, pp. 1375–1379, 2021.

[7] A. Biem, S. Katagiri, and B.-H. Juang, "Pattern recognition using discriminative feature extraction," *IEEE Transactions on Signal Processing*, vol. 45, no. 2, pp. 500–504, 1997.

[8] F. Bandiera, A. Farina, D. Orlando, and G. Ricci, "Detection algorithms to discriminate between radar targets and ecm signals," *IEEE Transactions on Signal Processing*, vol. 58, no. 12, pp. 5984–5993, 2010.

[9] S. Zhao, Y. Zhou, L. Zhang, Y. Guo, and S. Tang, "Discrimination between radar targets and deception jamming in distributed multiple-radar architectures," *IET Radar, Sonar & Navigation*, vol. 11, no. 7, pp. 1124–1131, 2017.

[10] D. Yao, Z. Liu, F. Li, and Y. Li, "Distorted sar target recognition with virtual svm and ap-hog feature," in *IET International Radar Conference*, 2020, pp. 734–739.

[11] L. Tian, Z. Zeng, Z. Li, and C. Liu, "Radar signal recognition method based on random forest model," in *2022 3rd International Conference on Big Data, Artificial Intelligence and Internet of Things Engineering (ICBAIE)*. IEEE, 2022, pp. 98–102.

[12] J. Zhang, M. Xing, and Y. Xie, "Fec: A feature fusion framework for sar target recognition based on electromagnetic scattering features and deep cnn features," *IEEE Transactions on Geoscience and Remote Sensing*, vol. 59, no. 3, pp. 2174–2187, 2020.

[13] L. Yongping, X. Ying, and B. Tang, "Smsp jamming identification based on matched signal transform," in *2011 International Conference on Computational Problem-Solving (ICCP)*. IEEE, 2011, pp. 182–185.

[14] Y. Wei, S.-R. Ou-Yang, C. Li, Q. Liu, and Y.-B. Qian, "Hierarchical jamming recognition with spectrum fusion feature and twin-bound SVM for cognitive satellite communications," in *2023 IEEE Wireless Communications and Networking Conference*. IEEE, 2023, pp. 1–6.

[15] D. Su and M. Gao, "Research on jamming recognition technology based on characteristic parameters," in *2020 IEEE 5th International Conference on Signal and Image Processing (ICSIP)*. IEEE, 2020, pp. 303–307.

[16] J. Lin and M. Gao, "Research on active jamming recognition method based on fractional fourier transform," in *2022 IEEE 6th Advanced Information Technology, Electronic and Automation Control Conference (IAEAC)*. IEEE, 2022, pp. 137–143.

[17] X. Chen, D. He, X. Yan, W. Yu, and T.-K. Truong, "GNSS interference type recognition with fingerprint spectrum dnn method," *IEEE Transactions on Aerospace and Electronic Systems*, vol. 58, no. 5, pp. 4745–4760, 2022.

[18] Y. Kong, X. Wang, C. Wu, X. Yu, and G. Cui, "Active deception jamming recognition in the presence of extended target," *IEEE Geoscience and Remote Sensing Letters*, vol. 19, pp. 1–5, 2022.

[19] J. Zhang, Z. Liang, C. Zhou, Q. Liu, and T. Long, "Radar compound jamming cognition based on a deep object detection network," *IEEE Transactions on Aerospace and Electronic Systems*, 2022.

[20] F. Auger and P. Flandrin, "Improving the readability of time-frequency and time-scale representations by the reassignment method," *IEEE Transactions on Signal Processing*, vol. 43, no. 5, pp. 1068–1089, 1995.

[21] Y. Junfei, L. Jingwen, S. Bing, and J. Yuming, "Barrage jamming detection and classification based on convolutional neural network for synthetic aperture radar," in *2018 IEEE International Geoscience and Remote Sensing Symposium*. IEEE, 2018, pp. 4583–4586.

[22] Q. Qu, S. Wei, S. Liu, J. Liang, and J. Shi, "Jrnet: Jamming recognition networks for radar compound suppression jamming signals," *IEEE Transactions on Vehicular Technology*, vol. 69, no. 12, pp. 15 035–15 045, 2020.

[23] J. Yang, Z. Bai, J. Hu, Y. Yang, Z. Xian, X. Hao, and K. Kwak, "Time-frequency analysis and convolutional neural network based fuze jamming signal recognition," in *25th International Conference on Advanced Communication Technology (ICACT)*. IEEE, 2023, pp. 277–282.

[24] Z. Lin, K. Ji, M. Kang, X. Leng, and H. Zou, "Deep convolutional highway unit network for sar target classification with limited labeled training data," *IEEE Geoscience and Remote Sensing Letters*, vol. 14, no. 7, pp. 1091–1095, 2017.

[25] Z. Zhang, Y. Li, Q. Zhai, Y. Li, and M. Gao, "Few-shot learning for fine-grained signal modulation recognition based on foreground segmentation," *IEEE Transactions on Vehicular Technology*, vol. 71, no. 3, pp. 2281–2292, 2022.

[26] Z. Wu, J. Qian, M. Zhang, Y. Cao, T. Wang, and L. Yang, "High-confidence sample augmentation based on label-guided denoising diffusion probabilistic model for active deception jamming recognition," *IEEE Geoscience and Remote Sensing Letters*, 2023.

[27] G. Shao, Y. Chen, and Y. Wei, "Convolutional neural network-based radar jamming signal classification with sufficient and limited samples," *IEEE Access*, vol. 8, pp.

80 588–80 598, 2020.

[28] Q. Lv, Y. Quan, W. Feng, M. Sha, S. Dong, and M. Xing, "Radar deception jamming recognition based on weighted ensemble cnn with transfer learning," *IEEE Transactions on Geoscience and Remote Sensing*, vol. 60, pp. 1–11, 2021.

[29] Z. Luo, Y. Cao, T.-S. Yeo, Y. Wang, and F. Wang, "Few-shot radar jamming recognition network via time-frequency self-attention and global knowledge distillation," *IEEE Transactions on Geoscience and Remote Sensing*, vol. 61, pp. 1–12, 2023.

[30] M. Liu, Z. Liu, W. Lu, Y. Chen, X. Gao, and N. Zhao, "Distributed few-shot learning for intelligent recognition of communication jamming," *IEEE Journal of Selected Topics in Signal Processing*, vol. 16, no. 3, pp. 395–405, 2021.

[31] L. Du, H. Liu, P. Wang, B. Feng, M. Pan, and Z. Bao, "Noise robust radar HRRP target recognition based on multitask factor analysis with small training data size," *IEEE Transactions on Signal Processing*, vol. 60, no. 7, pp. 3546–3559, 2012.

[32] Z. Luo, Y. Cao, T.-S. Yeo, and F. Wang, "Few-shot radar jamming recognition network via complete information mining," *IEEE Transactions on Aerospace and Electronic Systems*, vol. 60, no. 3, pp. 3625–3638, 2024.

[33] J. Wang and Y. Zhai, "Prototypical siamese networks for few-shot learning," in *2020 IEEE 10th International Conference on Electronics Information and Emergency Communication (ICEIEC)*. IEEE, 2020, pp. 178–181.

[34] S. Xiang, F. Nie, and C. Zhang, "Semi-supervised classification via local spline regression," *IEEE Transactions on Pattern Analysis and Machine Intelligence*, vol. 32, no. 11, pp. 2039–2053, 2010.

[35] L. Zhuang, Z. Zhou, S. Gao, J. Yin, Z. Lin, and Y. Ma, "Label information guided graph construction for semi-supervised learning," *IEEE Transactions on Image Processing*, vol. 26, no. 9, pp. 4182–4192, 2017.

[36] C. Zhao, X. He, J. Liang, T. Wang, and C. Huang, "Radar HRRP target recognition via semi-supervised multi-task deep network," *IEEE Access*, vol. 7, pp. 114 788–114 794, 2019.

[37] Y. Dong, X. Jiang, L. Cheng, and Q. Shi, "Ssrcnn: A semi-supervised learning framework for signal recognition," *IEEE Transactions on Cognitive Communications and Networking*, vol. 7, no. 3, pp. 780–789, 2021.

[38] K. Tan, W. Yan, L. Zhang, Q. Ling, and C. Xu, "Semi-supervised specific emitter identification based on bispectrum feature extraction cgan in multiple communication scenarios," *IEEE Transactions on Aerospace and Electronic Systems*, vol. 59, no. 1, pp. 292–310, 2022.

[39] F. Gao, W. Shi, J. Wang, A. Hussain, and H. Zhou, "A semi-supervised synthetic aperture radar (sar) image recognition algorithm based on an attention mechanism and bias-variance decomposition," *IEEE Access*, vol. 7, pp. 108 617–108 632, 2019.

[40] Z. Lian, B. Liu, and J. Tao, "Smin: Semi-supervised multi-modal interaction network for conversational emotion recognition," *IEEE Transactions on Affective Computing*, vol. 14, no. 3, pp. 2415–2429, 2023.

[41] K. Heidler, I. Nitze, G. Grosse, and X. X. Zhu, "Pixeldino: Semi-supervised semantic segmentation for detecting permafrost disturbances in the arctic," *IEEE Transactions on Geoscience and Remote Sensing*, vol. 62, pp. 1–12, 2024.

[42] X. Wang, S. Chen, Y. Zhu, S. Zhang, X. Li, and L. Zhu, "Application of wavelet scattering network and ensemble learning on deception jamming recognition for ultra-wideband detectors," *IEEE Transactions on Microwave Theory and Techniques*, pp. 1–11, 2023.

[43] N. Li, D. Cheng, P. Lu, G. Shu, and Z. Guo, "Smart jamming against sar based on nonlinear frequency-modulated signal," *IEEE Transactions on Aerospace and Electronic Systems*, vol. 59, no. 4, pp. 3588–3605, 2023.

[44] W. Wang, J. Wu, J. Pei, Z. Sun, J. Yang, and Q. Yi, "Antirange-deception jamming from multijammer for multistatic sar," *IEEE Transactions on Geoscience and Remote Sensing*, vol. 60, pp. 1–12, 2022.

[45] P. Sun, J. Yu, and W. Hao, "Research on radar active jamming recognition based on 2-d time-frequency features," in *2021 3rd International Academic Exchange Conference on Science and Technology Innovation (IAECST)*, 2021, pp. 777–781.

[46] K. Zhou, D. Li, Y. Su, and T. Liu, "Joint design of transmit waveform and mismatch filter in the presence of interrupted sampling repeater jamming," *IEEE Signal Processing Letters*, vol. 27, pp. 1610–1614, 2020.

[47] Z. Yanbin, "Technology of smart noise jamming based on multiplication modulation," in *2011 International Conference on Electric Information and Control Engineering*, 2011, pp. 4557–4559.

[48] S. Barbarossa, "Analysis of multicomponent lfm signals by a combined wigner-hough transform," *IEEE Transactions on Signal Processing*, vol. 43, no. 6, pp. 1511–1515, 1995.

[49] F. Millioz and N. Martin, "Circularity of the stft and spectral kurtosis for time-frequency segmentation in gaussian environment," *IEEE Transactions on Signal Processing*, vol. 59, no. 2, pp. 515–524, 2011.

[50] M. Yaseen, "What is YOLOv8: An In-Depth Exploration of the Internal Features of the Next-Generation Object Detector," *arXiv*, p. arXiv:2408.15857, Aug. 2024.

[51] A. H. Khan, X. Cao, S. Li, V. N. Katsikis, and L. Liao, "Bas-adam: An adam based approach to improve the performance of beetle antennae search optimizer," *IEEE/CAA Journal of Automatica Sinica*, vol. 7, no. 2, pp. 461–471, 2020.

[52] P. Shivakumara, S. Bhowmick, B. Su, C. L. Tan, and U. Pal, "A new gradient based character segmentation method for video text recognition," in *2011 International conference on document analysis and recognition*. IEEE, 2011, pp. 126–130.

[53] L. Zhang, Z. Zhang, C. L. Tan, and T. Xia, "3D geometric and optical modeling of warped document images from scanners," in *2005 IEEE Computer Society Conference on Computer Vision and Pattern Recognition (CVPR'05)*, vol. 1. IEEE, 2005, pp. 337–342.

[54] Y. Li, Z. Zhang, F. Zhou, Y. Xing, J. Li, and C. Liu, "Multi-label classification of arrhythmia for long-term electrocardiogram signals with feature learning," *IEEE Transactions on Instrumentation and Measurement*, vol. 70, pp. 1–11, 2021.

[55] C. Sui, Y. Tian, Y. Xu, and Y. Xie, "Unsupervised band selection by integrating the overall accuracy and redundancy," *IEEE Geoscience and Remote Sensing Letters*, vol. 12, no. 1, pp. 185–189, 2015.